Generation of Quasiperiodic Order by Maximal Cluster Covering

Franz Gähler, Petra Gummelt, and Shelomo I. Ben-Abraham

1 Introduction

In quasicrystals, certain structural motifs occur very frequently, and sometimes even cover the entire structure. This property is particularly visible in high resolution electron micrographs (HREMs) of decagonal quasicrystals. In the context of this article, these important structural motifs will be called *clusters*.[1] Based on the observation that at least some quasicrystals can be regarded as being covered by a single kind of cluster, Burkov [1] was one of the first to propose a structure model which was explicitly given as a covering with overlapping copies of a single cluster.

The Burkov model mostly remained at the descriptive level. However, if a cluster occurs so frequently that it covers the entire structure, it must certainly be an energetically favourable local configuration. Moreover, the many overlaps, which necessarily occur if the entire structure is covered, impose constraints on the possible relative positions and orientations of the clusters. Overlapping clusters will share the atoms in the overlap, and thus have to agree in the overlap region. This can severely limit the number of possible overlaps. Generally speaking, the constraints on the possible overlaps create order.

Based on such ideas, Jeong and Steinhardt [2] have formulated a simple ordering principle which can produce a perfectly ordered quasicrystal. They suggested that a quasicrystal will try to maximize the density of the most favourable local configurations (clusters), and thus effectively expels all the other local configurations which do not occur in the perfect structure. They could show by Monte Carlo simulations that favouring just the few most important local motifs can produce a perfectly ordered Penrose tiling. This ordering principle will be called the *cluster density maximization principle*.

Having such a simple model for the energetics of a quasicrystal, which is still able to produce a perfectly ordered structure as its ground state, is a clear advantage over earlier models based on matching rules [3], or local rules [4], as they are sometimes called. Matching rules consist of an atlas of all those local configurations, up to a radius R, which can occur in the ordered

[1] Note that these clusters are embedded in the surrounding quasicrystal, and should not be confused with finite clusters in vacuum.

quasicrystal structure. This atlas must have the additional property that every structure containing only local configurations from the atlas is perfectly ordered. The minimal radius R for which an atlas with these properties exists is called the range of the matching rules. An atlas with these properties (and thus matching rules) need not always exist for any R, but there are many examples of quasiperiodic tilings which do have matching rules [5–8]. Quasicrystals can often be regarded as being an atomic decoration of such a tiling. There is an obvious way to use matching rules to construct a simple energetics for the corresponding tiling model of a quasicrystal. One just has to make sure that all allowed local configurations (those occuring in the atlas) are energetically more favourable than all other possible local configurations. However, such an atlas usually contains very many local configurations, and trying to realize such interactions for the *atoms* which decorate the tiles is a hopelessly complicated task.

The cluster model approach of Jeong and Steinhardt [2] suggests that it is not necessary that all allowed local configurations have lower energy than all disallowed local configurations. Preferring just the most important motifs, and ignoring all the rest, can be enough to produce an ordered quasicrystal. This is a tremendous simplification over the more naive matching rule approach. Nevertheless, it is still a non-trivial task to select the right clusters which can produce an ordered ground state. Such clusters must be sufficiently restrictive on the overlaps they admit. In this respect, *asymmetric* clusters work much better, and it is interesting to note that asymmetric clusters seem to be preferred by the electronic structure in decagonal quasicrystals [9]. Morever, the clusters must be big enough. In fact, it has been shown [10] that their size can be no smaller than the range of the matching rules.

While Jeong and Steinhardt suggested to maximize the *density* of certain well-chosen clusters, a slightly different approach was proposed by Gummelt [11,12], who presented a decagon with associated overlap rules having the property, that every covering of the plane with this decagon obeying the overlap rules is isomorphic to a perfectly ordered Penrose tiling. This decagon, together with its overlaps rules, will in the following be called the *aperiodic decagon*. This result was an important progress in two respects. Firstly, a *single* cluster (the decagon) with overlap rules was sufficient to produce a perfectly ordered structure, and secondly, the cluster density maximization principle was replaced by a *cluster covering principle*, which from a mathematical point of view is much easier to handle. Indeed, the properties of the aperiodic decagon can all be proved mathematically, whereas the results of Jeong and Steinhardt [2] where supported only by simulations. The fact that the properties of the aperiodic decagon are mathematically well established probably had a further effect, perhaps together with the extraordinary beauty of the model. It has encouraged many researchers [13–17] to interpret their HREM images using models based on the aperiodic decagon, thus providing an extraordinary impetus to the field. The aperiodic decagon can be used also together with the cluster density maximization principle. Jeong and Steinhardt [18] could show that the perfect Penrose tiling has a decagon cluster density no smaller than any other tiling, whether it is covered or not.

As we have already indicated above, the cluster density maximization principle is a particularly efficient realization of the matching rules of a tiling or quasicrystal. The same is obviously the case also for the cluster covering principle. This idea can be pushed even a little further. Many tilings have very complicated matching rules. This is particularly so for octagonal and dodecagonal tilings [6–8]. These matching rules require decorations of the tiling which are not locally derivable [19] from the undecorated tiling [8]. There is, however, a simple subset of the matching rules for these tilings, the so-called *alternation condition* [20], which is local also for the undecorated tiling, and which enforces perfectly ordered tilings, albeit ones which in general have lower symmetry [21]. In this situation, a combination of the cluster density maximization principle and the cluster covering principle can be used. In a first step, the alternation condition is enforced by a suitable cluster covering principle. In a second step, the fully symmetric octagonal or dodecagonal tiling can then be selected as the one with the highest cluster density, but only among the tilings which are completely covered by the cluster. This will be called the *maximal cluster covering principle*. It can use relatively simply clusters at the expense of a more refined ordering principle. The maximal covering principle was used for octagonal tilings implicitly already in [22], and more explicitly in [23]. Recently, it could be applied also to dodecagonal tilings [24].

We have therefore three simple *ordering principles* for quasicrystals, which can produce a perfectly ordered quasicrystal. The structure of the quasicrystal is selected according to one of the following rules:

- require that the structure maximizes the density of some well-chosen cluster(s);
- require that the structure is covered by some well-chosen cluster(s);
- require that the structure is covered by the cluster(s), and among these take the ones with the highest cluster density.

These ordering principles are clearly closely related, but conceptually distinct. In some cases, all three may be applied, but in other cases only the third one will work. Conceptually, they all have their advantages and disadvantages. If an energy function simply counts the number of (overlapping) clusters, there is clearly some double-counting, which should be avoided or compensated. The covering principle may be better suited in this respect. It basically requires that *every* atom is contained in some energetically favourable local configuration. The maximal cluster covering principle is a further refinement: it requires a cluster *covering*, but prefers among those the ones with the higher cluster density. In a covering with higher cluster density, it is more likely that atoms are well in the interior of some cluster, which might be better than just on the cluster surface.

We should emphasize that the notion of covering may have different definitions, depending on the context. In the context of a tiling, by a covering of the tiling we usually mean that all tiles of the tiling are covered by copies of a tile cluster, but there are other possibilities. For instance, a covering of a tiling could also mean that all vertices of the tiling are covered by a vertex cluster. The general concepts are very flexible, and one has to define in each particular case what exactly shall be the meaning of a covering. In the case of an atomic structure, a cluster covering usually means that every atom in the structure is part of at least one of the atom clusters. In other words, it is the set of atoms which shall be covered. Even with this understanding of a covering, there may still be variants of the covering concept. In this article, we require that two atom clusters completely agree in the overlap region. In other words, any atom in the overlap region must be part of both clusters involved. Of course, this requires a suitable definition of overlap region. Other authors use a looser notion of matching in the overlap region of two clusters. In [9,17,18], for instance, cluster overlaps are also admissible if not all atoms in the overlap region of two clusters are part of both clusters. This may make it difficult to compare different models, and statements that the overlap rules imposed by an atomic cluster are equivalent to, e.g., those of the aperiodic decagon, have to be taken with a grain of salt, if it is not clearly defined under which condition two overlapping clusters shall be compatible with each other.

We should also note that our ordering principles do not specify which cluster is the right one. The emphasis of this article will be precisely on this question: which clusters can produce, by means of the above ordering principles, a perfectly ordered quasicrystal, or at least some other 'interesting' class of structures, and which tilings (and related quasicrystals) admit such clusters. Our goal is therefore not merely to describe a given quasicrystal structure in terms of a cluster covering, but rather to determine the class of structures admitted by a given set of overlap rules, which is imposed by the internal structure of the clusters that have been chosen for the covering.

It is clear that not every cluster we may chose can lead to a perfectly ordered quasicrystal. Much more typical is the converse. Very often, a cluster either cannot cover any interesting structure completely, or it can cover too many. The latter case can still be interesting. In such cases, the structures that can be covered are typically members of some *super-tile random tiling* ensemble [2,22]. Super-tile random tilings consist of larger, inflated tiles (the super-tiles), whose interior is ordered, but which are arranged randomly, forming a random-tiling [25]. On a local scale, such structures look ordered; only at larger scales one can notice the disorder. Since real quasicrystals are not all perfectly quasiperiodic, clusters selecting a entire super-tile random tiling ensemble can be very relevant. It has even been proposed [26,27] to relax overlap rules known to produce a perfectly ordered quasicrystal, in order to allow for a larger class of structures, including ones containing some amount of disorder.

After introducing our principal tools in Sect. 2, most of the remainder of this article is a detailed discussion of the available results related to several two-dimensional quasiperiodic tilings, as well as the quasicrystal models built upon them. In particular, we shall discuss the decagonal Penrose tiling [5] and several other tilings related to it (Sect. 3), the octagonal Ammann-Beenker tiling [6,28,29] (Sect. 4), and the dodecagonal Socolar [6] and shield [30,31] tilings (Sect. 5). Finally, we put these results into a more general context in Sect. 6, where we comment also on the case of the Tübingen Triangle Tiling (TTT) [32]. Each of these models sheds some light on a different aspect of the general principles. Reviews of some parts of these results have appeared already earlier [33,34].

2 Important Concepts and Tools

In this section we briefly review the principal concepts and tools needed to obtain the results presented in this article. The most important tool certainly is the concept of *mutual local derivability* (MLD) [19], sometimes also called *local equivalence*. Mutual local derivability is a local equivalence relation between tilings, or other discrete structures like a Delone set, or the set of atom positions in a quasicrystal, including labels for the different chemical species. In order to be specific, we explain the concept for tilings.

Consider two tilings, $\mathcal{T}_1$ and $\mathcal{T}_2$, which are assumed to be embedded in the same space with fixed position, orientation, and scale. Tiling $\mathcal{T}_1$ is said to be locally derivable from tiling $\mathcal{T}_2$, if there exists a fixed $\delta < \infty$ such that every patch $P_{R,x}(\mathcal{T}_1)$ of $\mathcal{T}_1$, with radius R and center x, is uniquely determined by the corresponding patch $P_{R+\delta,x}(\mathcal{T}_2)$. In this definition, the *derivability radius* δ must be independent of R and x. Loosely speaking, tiling $\mathcal{T}_1$ can be constructed from tiling $\mathcal{T}_2$ using local knowledge only. If $\mathcal{T}_2$ is also locally derivable from tiling $\mathcal{T}_1$, possibly with a different derivability radius δ, the two tilings are said to be mutually locally derivable (MLD). MLD clearly is a (local) equivalence relation.

Another important equivalence concept for discrete structures like tilings is that of *local isomorphism* (LI). Two tilings are said to be locally isomorphic, if any finite patch of one tiling occurs also somewhere in the other, and vice versa. All tilings locally isomorphic to a given one form the local isomorphism class (LI class) of that tiling. It is immediately clear from the definitions of local isomorphism and mutual local derivability, that if two tilings are MLD, then this equivalence relation can be extended to a bijection between the respective LI classes of the tilings. To each tiling $\mathcal{T}_1$ in the first LI class, there exists a unique tiling $\mathcal{T}_2$ in the second LI class, such that the two tilings are MLD. Abusing a bit the language, we then say that the two LI classes are MLD. The MLD concept can even be extended to more general classes of tilings. One can think of two ensembles of random tilings, such that for each tiling in one ensemble there is a unique partner tiling in the other ensemble which is MLD with it, and vice versa. We then say that the two ensembles are MLD. Note that in the case of mutual local derivability between such general ensembles of tilings, one should also require that the derivability radius δ is uniformly bounded over the ensembles. This extra requirement is not necessary for the LI class of a tiling, where δ is automatically constant over the LI class. In many examples, the MLD concept can be used in this way to relate a new random tiling ensemble, or a new random covering ensemble, to other random tilings ensembles already known from the literature.

If two ensembles of tilings are MLD, many properties depending only on *local* information on the tilings can easily be transferred from one ensemble to the other. An important example of such a property is the existence of *matching rules*. A tiling $\mathcal{T}$ (or other discrete structure) is said to have matching rules of radius R, if any other tiling with the property, that all its patches of radius R occur also in $\mathcal{T}$, is locally isomorphic with $\mathcal{T}$. In other words, the LI class of $\mathcal{T}$ is completely determined by the R-patches of $\mathcal{T}$ for some *finite* R. Note that such a finite atlas can never distinguish between different members of an LI class. Matching rules are therefore always matching rules for an LI class. It is clear that if two LI classes are MLD with derivability radius δ, and one has matching rules of radius R, then the other also must have matching rules, of radius not bigger than $R + \delta$. Examples where such concepts have been applied to transfer matching rules from one tiling to another can be found in [35].

Unfortunately, it is not always possible to relate a tiling ensemble of interest to something else which is already known in all details. This is so in particular for random tiling ensembles. In such cases, a further important tool is that of Monte Carlo simulations. Such simulation methods are needed, in particular, for the study of cluster density maximization models, where it is very difficult to prove anything rigorously. Monte Carlo simulations can for instance be used to search for the tilings with highest cluster density within some larger tiling ensemble. For this purpuse, an energy function is defined on the space of tilings, which gives the lowest energy to the tilings with the highest cluster density. One then simulates a tiling ensemble at temperature T, and by slow cooling (simulated annealing) one can reach the states with lowest energy. We can not go into the details of these simulation techniques here, but refer for a general background to [36].

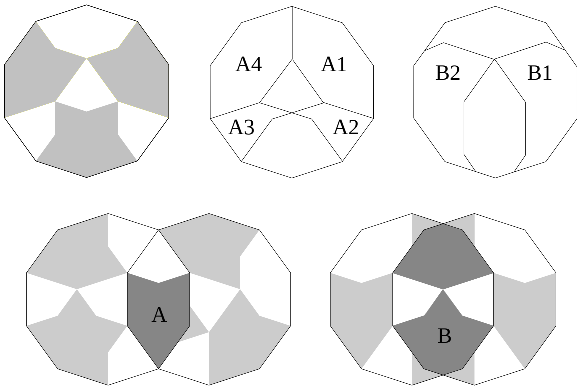

Fig. 1. Aperiodic decagon **(top left)**, with the allowed overlap zones for A- and B-overlaps (**top middle and right**), and representative A- and B-overlaps (**bottom**)

3 Penrose and Related Tilings

3.1 Perfect Decagon Coverings

The aperiodic decagon introduced by Gummelt [11,12] provides the first and most striking example where perfect quasiperiodic order can be obtained by a simple cluster covering principle. The overlap rules for the decagons is encoded in their shading: if two decagons overlap, their shadings must agree in the entire overlap region (Fig. 1). A patch of decagons satisfying the overlap rules is shown in Fig. 2. These simple overlap rules are capable of enforcing a structure isomorphic to a perfect Penrose tiling. More precisely, the set of decagon coverings of the plane obeying the overlap rules is MLD with the set of perfect Penrose tilings. In other words, there is a one-to-one correspondence beween decagon coverings and Penrose tilings, and this correspondence is local.

We can here only sketch the proof of this statement. It requires a detailed analysis of those local decagon arrangements which can be extended to a complete covering. This analysis has been carried out in [12]. It is straightforward, but somewhat tedious. The first important result of this analysis is, that a local decagon arrangement can be continued to a full covering of the plane only if all decagon overlaps are of only two types, A and B (Fig. 1). Moreover, these overlaps can occur only in certain overlap zones (Fig. 1). If other overlaps occur, even if they satisfy the condition of a matching shading, the decagon arrangement cannot be extended to a covering of the entire plane. Next, it has been shown that there is a one-to-one correspondence between local decagon arrangements in a covering and local tile arrangements in a Penrose tiling. This correspondence is indicated in Fig. 3 for a Penrose rhombus tiling (note that near the decagon boundary some edges of the Penrose tiling are not fully specified; these edges depend on the presence or absence

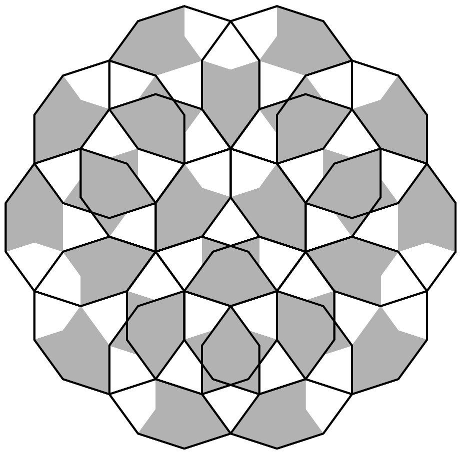

Fig. 2. A patch of an aperiodic decagon covering. The shading allows two kinds of decagon overlaps

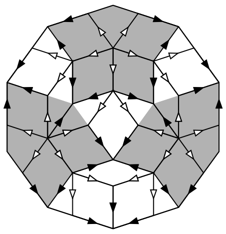

Fig. 3. Aperiodic decagon, superimposed with corresponding patch of a Penrose tiling

of neighboring decagons). This correspondence has been established for all decagon arrangements whose decagons contain some commen point. These local decagon arrangements are large enough so that one can then make use of the (short-range) matching rules of the Penrose tiling: every tiling that looks locally, at the scale of these finite decagon arragements, like a Penrose tiling, is indeed a Penrose tiling.

From the proof sketched above it becomes clear that the decagon overlap rules are really just an efficient reformulation of the Penrose matching rules. Using MLD concepts, the matching rules, which are called overlap rules in the covering context, can be transferred from one system to the other, and vice versa. The proof given in [12] has later been simplified somewhat [18], but the basic idea is still the same.

In the original formulation, the aperiodic decagon is an example of the cluster covering principle. Jeong and Steinhardt [18] could show, however, that among all tilings with the two Penrose rhombi, the Penrose tiling is the one with the highest density of the tile cluster corresponding to the aperiodic decagon. This holds true, in particular, also for tilings which are not covered by this cluster. Therefore, the cluster density maximization principle can also be used in this case, although it is mathematically much more difficult to obtain any rigorous results.

In the description above we have related the decagon coverings to the Penrose rhombus tilings. There are several other kinds of Penrose tilings [37], such as kite-and-dart Penrose tilings, Penrose tilings by Robinson triangles, and Penrose tilings with pentagons, rhombi, ship- and star-shaped tiles. All these tilings are MLD with each other, and so they are MLD with the decagon coverings. Instead of the Penrose rhombus tilings, any other kind of Penrose tilings could have been used to establish the relationship to decagon coverings [38]. In Sect. 3.2, it will be advantageous to use Penrose pentagon tilings rather than rhombus tilings.

Coverings by the aperiodic decagon have found many applications in the description of the structure of decagonal quasicrystals, and many authors have attempted to explain the stability and existence of these quasicrystals by a cluster covering principle [9,13–17]. The equivalence of the decagon overlap rules and those implied by the atomic structure of the clusters involved is not always completely evident, however. One reason is that it is not always clearly stated which overlaps of the clusters shall be considered admissible.

3.2 Random Decagon Coverings

In Sect. 3.1 we have seen how a perfect Penrose tiling (and associated quasicrystals) can be obtained with a simple cluster covering principle. However, many experimental decagonal quasicrystal structures are not perfectly quasiperiodic, and it is therefore interesting to consider also overlap rules which are less restrictive than those for the aperiodic decagon, and which do not enforce a perfectly ordered structure, but rather a (super-tile) random tiling structure. The analysis of such relaxed overlap rules and their corresponding structures will be the subject of most of the rest of Sect. 3. Most of these results have been presented in [27].

Before we start the discussion of the relaxed overlap rules, we have to recall one further fact on perfect decagon coverings. In Sect. 3.1, we have established the relation between decagon coverings and Penrose rhombus tilings. For the transition to relaxed overlap rules, it is more natural to use Penrose pentagon tilings (PPTs), however. These consist of pentagons, rhombi, ship- and star-shaped tiles. It has been shown [12] that the decagon centers of a decagon covering obeying the perfect overlap rules form the vertex set of a PPT, and that every PPT can be obtained in this way from exactly one covering satisfying the perfect overlap rules. This is the MLD correspondence between perfect decagon coverings and PPTs. It is a one-to-one correspondence, and it is local. As the aperiodic decagon represents a cluster in the corresponding quasicrystal, we will often also use the term cluster for the covering decagon.

In order to allow for partially disordered coverings, Gummelt and Bandt [26] have proposed to relax the overlap rules of the aperiodic decagon to some extent. To understand the type of relaxation, recall that if the perfect rules are obeyed, a decagon may have small A-overlaps with neighbor decagons in four possible directions, and bigger B-overlaps with neighbor decagons in two possible directions (Fig. 1). The coloring in the overlap region has an orientation, which must be respected. All possible overlaps are therefore *oriented*. As a relaxation of the perfect rules, Gummelt and Bandt have now proposed [26] to abandon this orientation constraint, and to retain only the condition which specifies the possible *overlap zones*, without orientation inside. These overlap rules will be referred to as the fully relaxed rules.

There is a natural intermediate between the perfect rules and the fully relaxed rules. In these rules, which will be just called the *relaxed rules*, the orientation condition is abandoned only for the small A-overlaps, but is retained for the larger B-overlaps. These intermediate rules and the resulting structures will be the main topic in the following.

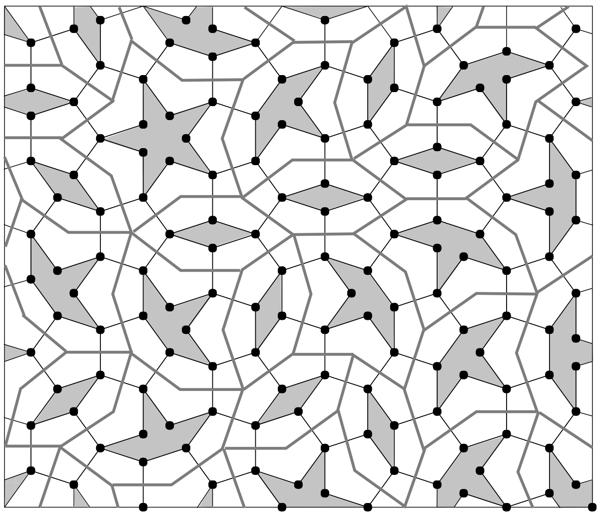

Fig. 4. Random Penrose pentagon tiling. Spiky tiles (shaded in gray) are surrounded by pentagons. This tiling is equivalent to a HBS tiling (drawn in gray), whose tile edges connect centers of neighboring pentagons

Using an analysis of all admissible local decagon arrangements as for the aperiodic decagon, Gummelt and Bandt have shown [26] that every covering satisfying the fully relaxed rules has the property that its set of cluster centers forms the vertex set of a random PPT having the additional property that all the spiky tiles (stars, ships, and rhombi, shaded in gray in Fig. 4) are completely surrounded by pentagons (in the following, when we say random

PPT, we always mean one satisfying this extra condition; more general ones won't play any role here). Such a random PPT is MLD to a random hexagon-boat-star (HBS) tiling, drawn in gray in Fig. 4. Since coverings satisfying the more restrictive relaxed rules satisfy also the fully relaxed rules, their set of cluster centers also forms the vertex set of a random PPT. Conversely, it is easy to see that every random PPT can arise both from relaxed and from fully relaxed coverings. The only difference between relaxed and fully relaxed coverings is the number of coverings associated with a given random PPT.

To see this, we note that the orientation of a cluster is already determined by the presence of two B-neighbors, or the presence of four A-neighbors. In Fig. 4 we see that A-neighbors are separated by an edge of a tile, or a long diagonal across a ship or a star, whereas B-neighbors are separated by a short diagonal of a rhombus, ship, or star. The only vertices whose cluster orientation is not fixed by the tiling are the obtuse corners of the rhombi, where two cluster orientations are possible. For the fully relaxed rules, where no orientation conditions are to be observed, we therefore have altogether four choices per rhombus for the cluster orientations.

For the relaxed rules, which have to obey the orientation condition for the B-overlaps, one can easily verify that the orientation condition for B-overlaps across ships and stars is always satisfied. In order that the same is true for B-overlaps across rhombi, however, the orientation of the cluster on the obtuse rhombus corners can not be chosen independently. The orientation condition is satisfied only for two of the four possible combinations.

Summarizing, for a given random PPT we have four independent choices per rhombus for a fully relaxed cluster covering, and two choices per rhombus for a relaxed cluster covering. In the same way, one can quantify the relationship between the cluster coverings and certain variants of a random Penrose rhombus tiling. The random HBS tilings arise from random Penrose rhombus tilings which still satisfy the double arrow condition [25,39]. Such random Penrose rhombus tilings are also called 4-level (or 4-vertex) Penrose random tilings. The double arrowed edges of the 4-level random Penrose tilings are simply wiped out to obtain the HBS random tilings, which are also known as 2-level Penrose tilings [25]. The relationship between 4-level and 2-level Penrose random tilings is not one-to-one: whereas the subdivision of boats and stars is unique, there are two choices for the subdivision of each hexagon into rhombi, just as there are two possible cluster assignments on the obtuse rhombus corners in the PPT. Since rhombi in the PPT and hexagons in the HBS tiling are in one-to-one correspondence, this implies that the multiplicity of relaxed cluster coverings and 4-level Penrose random tilings related to a given random PPT is the same.

3.3 Cluster Density Maximization

In Sect. 3.2 we have considered cluster *coverings*, where our clusters have simply been decagons with certain overlap rules. Another variant of the ordering

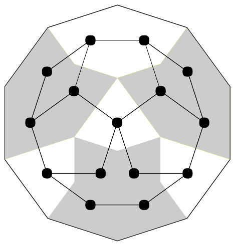

Fig. 5. Vertex cluster superimposed on aperiodic decagon. This cluster enforces the relaxed overlap rules

principle is *cluster density maximization*. The relaxed overlap rules allow for a very natural realization in terms of a vertex cluster in a random PPT (we still require that spiky tiles are completely surrounded by pentagons). This vertex cluster is shown in Fig. 5, superimposed on the aperiodic decagon. The tile edges are drawn only as a guide to the eye; they are not part of the cluster, only the vertex set counts. It is easy to see that the orientation of the A-overlaps of the aperiodic decagon can not be enforced by the vertex set of the cluster, whereas the orientation of the B-overlaps is enforced. The A-overlap consists of a rhombus, and the B-overlap of a hexagon with an extra vertex in asymmetric position inside.

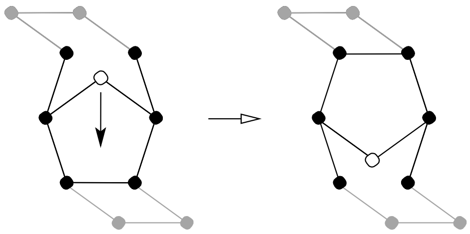

Fig. 6. Flip move for Monte Carlo simulation

With this cluster we can now build a statistical model of cluster density maximization. We consider the set of all random PPTs, and assign a weight to each tiling, which is simply the number of vertex clusters it contains. With Monte Carlo simulations it is then possible to find the subensemble of those random PPTs which have maximal cluster density. For the simulations we will need a Monte Carlo dynamics which is ergodic in the ensemble of all random PPTs. We have found that the flip move shown in Fig. 6 has the required properties. By repeated flips it is possible to turn any random PPT into any other. One must be careful, however, not to execute any flips which would introduce new kinds of tiles. This can be avoided if some local constraints on the flips are obeyed.

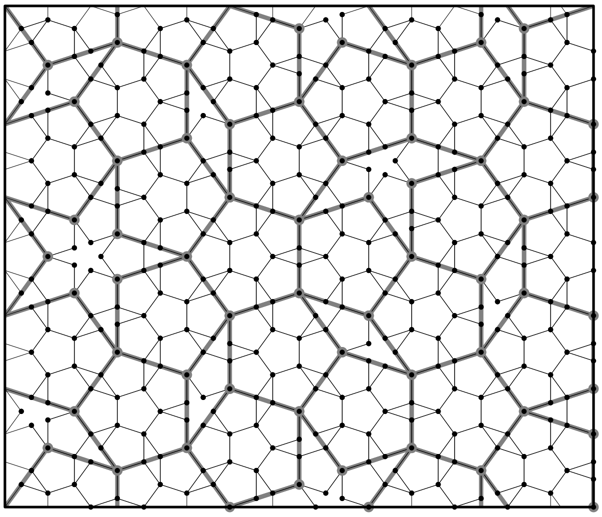

Fig. 7. Structure with maximal cluster density. The cluster centers form the vertices of a super-tile random PPT

With such a Monte Carlo model, the states of maximal cluster density have been determined with simulated annealing, using as energy function the negative of the number of clusters, thus mimicking the total cohesion energy of the clusters. It turns out that these states of maximal cluster density are precisely the super-tile random PPTs, whose tiles have an edge length τ^2 times that of the small tiles, where $\tau = (1 + \sqrt{5})/2$ is the golden ratio. An example of such a super-tile tiling is shown in Fig. 7. In view of the results of Sect. 3.2, this is of course not too surprising. The cluster centers sit on the vertices of the super-tile tiling, covering all vertices of the small tiles. Since the vertex cluster is smaller than the aperiodic decagon, it does not cover the whole area, but only the vertices. There remain small pentagons uncovered, which sit at the center of the super-tile pentagons. This does not affect the overlap constraints, however. Our results therefore imply that there is a one-to-one MLD correspondence between cluster coverings satisfying the relaxed rules, and structures with maximal density of the vertex cluster. Although these two ordering principles are very similar, they are conceptually slightly different and must be distinguished.

3.4 Entropy Density

With the cluster model of Sect. 3.3, it is also possible to measure the entropy density of the ensemble of structures with maximal cluster density, and thus the entropy density of the relaxed cluster covering ensemble. We have an energy model which assigns a cohesion energy to each cluster in the structure. In this model, the ground state, the state of maximal cluster density, consists

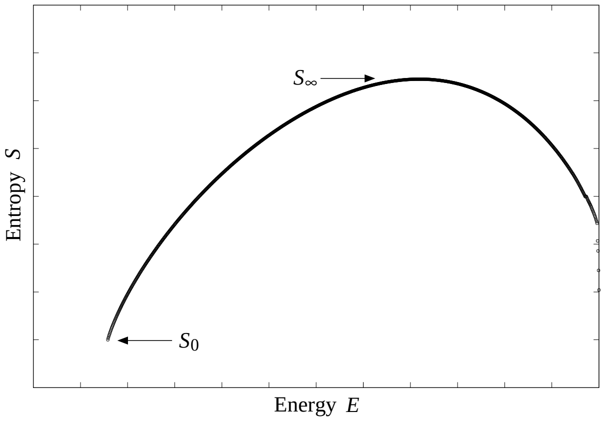

Fig. 8. Entropy as a function of energy for a selected approximant

of super-tile random PPTs, with an extra weight of two per rhombus, because for each rhombus there are two choices of a cluster configuration with the same number of clusters. At infinite temperature, on the other hand, we have the full random PPT (with the small tiles). With entropic sampling techniques [40,41], it is now possible to determine the entropy of the system as a function of energy, and in particular the difference in entropy between the ground state and the infinite temperature state. An example of such an entropy function is shown in Fig. 8. The entropy of the ground state can be extracted in the following way. The entropies at zero and infinite temperature are both entropies of random PPTs, once with and once without extra degeneracy for each rhombus. Moreover, the two random tilings are at different scales. Taking both differences into account, we arrive at the following relation for the two entropy densities:

$$\sigma_0 = \tau^{-4}(\sigma_\infty + \rho_{\mathrm{rh}} k_{\mathrm{B}} \ln 2) \tag{1}$$

where ρ_{rh} is the measured rhombus density in the high temperature state. If we now write $\sigma_\infty = \sigma_0 + \Delta\sigma$, we obtain an equation for the ground state entropy denstiy σ_0, in which all other quantities are known. The ground state entropy density has been determined in this way for several periodic approximants. By finite size scaling, this can then be extrapolated to infinite system size. This is shown in Fig. 9, where one can see that the scaling works very nicely. At a scale where the super-tile edges (which separate A-overlap neighbors in the cluster model) have unit length, we obtain a value of

$$\sigma_0/k_{\mathrm{B}} = 0.253 \pm 0.001 \tag{2}$$

for the entropy density. This value can be compared with the value Tang and Jarić [39] have obtained for the entropy density of the 4-level random Penrose tiling. In Sect. 3.2 we have seen that 4-level random Penrose tilings are in one-

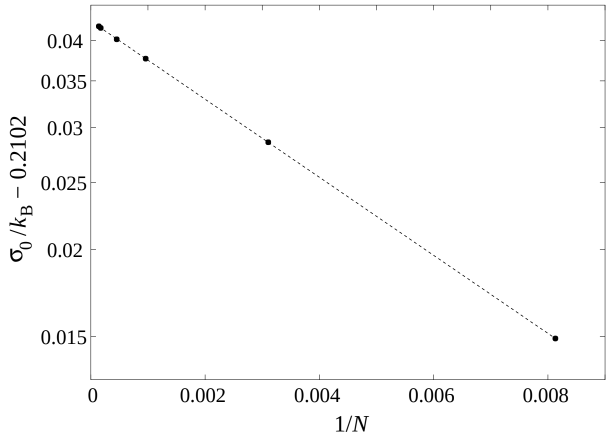

Fig. 9. Finite size scaling of the entropy density

to-one correspondence with relaxed cluster coverings. If the different scales of the two tilings are corrected for, Tang and Jarić obtained a value of

$$\sigma_0/k_\mathrm{B} = 0.255 \pm 0.001 \tag{3}$$

which is compatible with ours.

3.5 Couplings Between Clusters

The only difference between the perfect and the relaxed overlap rules is that the latter do not require *oriented* A-overlaps. Since not all relaxed coverings are perfect, there must be A-overlaps in an relaxed covering which do not obey the orientation condition of the perfect rules. A closer analysis shows [26] that there is actually only one kind of disoriented A-overlap which can actually occur in a relaxed covering. If we represent the orientation of a cluster on a vertex of a super-tile PPT by an arrow, we can represent the covering in a much more compact way, as shown in Fig. 10. The disoriented A-overlaps not permitted by the perfect rule are marked in Fig. 10. The corresponding tile edges have antiparallel arrows at their ends.

This representation suggests to introduce a coupling of neighboring clusters in such a way that overlaps which are not permitted by the perfect rules are energetically penalized. We expect such a coupling to be weak, because these kinds of defects can be detected only at larger scales. However, at low enough temperature it might still be able to order the super-tile random tiling ground state of the relaxed cluster covering to a perfectly ordered structure. This suggests a scenario with two energy scales: the presence of each vertex cluster lowers the cohesion energy by a large amount, so that structures with maximal cluster density are strongly favoured, even at relatively elevated temperature. The equilibrium structures at these temperatures are therefore relaxed cluster coverings. Additionally, there is a small coupling between

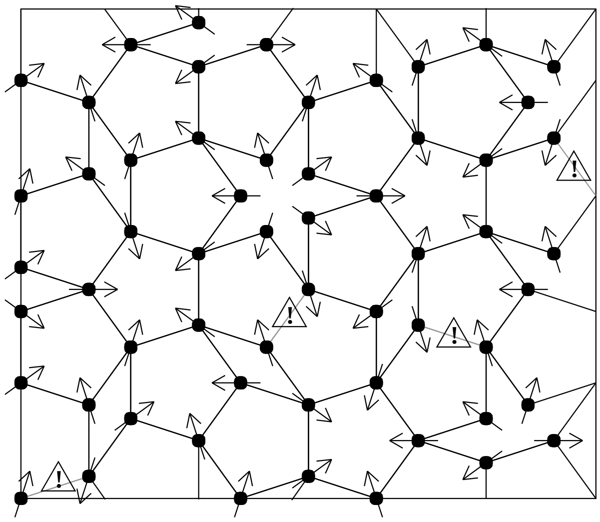

Fig. 10. Super-tile tiling with cluster orientations indicated by arrows

neighboring clusters, which at low temperatures can order the super-tile random tiling to a perfectly ordered tiling.

We have verified the feasibility of this model by Monte Carlo simulations. Our model considers only the subensemble of states with maximal cluster density. In other words, we simulate at the level of the super-tile tiling. The cluster on each vertex is represented by an arrow, like in Fig. 10. This setup keeps the number of clusters constant, so that we cannot leave the states of maximal cluster density, which simplifies the simulation considerably. As flip move we can still use the one of Fig. 6, except that here we have to adjust the cluster orientations of the neighboring vertices of the flip to new values consistent with the new tile configuration. Additionally, we have to introduce a new type of flip, which only changes the cluster orientations on the obtuse corners of a rhombus, but keeps the tiling fixed.

With this model, we have verified that the coupling of the clusters can indeed order the model to a perfectly quasiperiodic structure. In other words, the ground state is a perfect quasicrystal, whereas the high temperature state is the super-tile random tiling with the additional degeneracy of the cluster orientations on the obtuse corners of the rhombi, corresponding to the relaxed cluster coverings. In this respect, high temperature means high compared to the cluster coupling, but still low compared to the energy required to break up clusters.

Also in this model it is possible to measure the entropy density of the relaxed covering ensemble. In this case, the ground state is ordered and has zero entropy (at least in the thermodynamic limit), and the high temperature state is the one whose entropy we are interested in. We therefore need only to measure the difference between the entropies of the high temperature state and the ground state, and extrapolate to the thermodynamic limit. It turns out, however, that finite size scaling for the present model does not work as well as for the model with a random tiling ground state. The results are therefore less precise, although they are consistent with the results reported in Sect. 3.4. We therefore won't present any details here.

3.6 An Atomic Cluster Enforcing the Relaxed Overlap Rules

We conclude Sec. 3 by showing that the relaxed overlap rules are very natural. We already have seen that they are equivalent to the natural overlap constraints of a simple vertex cluster. There is, however, also a natural atomic cluster enforcing essentially the same overlap constraints. This cluster has been found by Roth and Henley [42] in a molecular dynamics simulation of decagonal Frank-Kasper type quasicrystals. It is shown in Fig. 11. The atoms drawn in black (which constitute one layer of the structure) form the vertices of a PPT. The only discrepancy with the overlap constraints of our vertex cluster is at the center of a star tile, where we would have expected a single atom at $z = 0$, not two atoms at $z = \frac{1}{4}, \frac{3}{4}$ (Fig. 11).

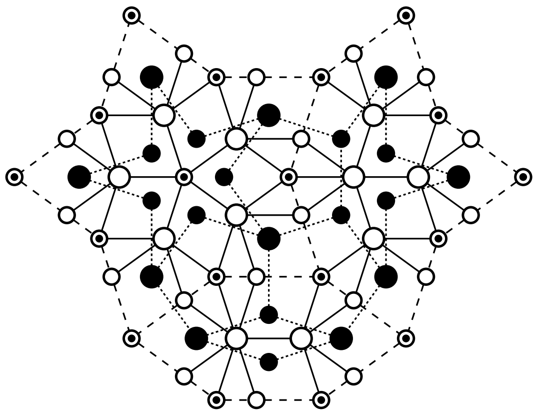

Fig. 11. Atomic cluster found by Henley and Roth [42] in a molecular dynamics simulation. In units of the period in the z-direction, white atoms are at $z = 0$, black atoms at $z = \frac{1}{2}$, and dotted atoms at $z = \frac{1}{4}, \frac{3}{4}$

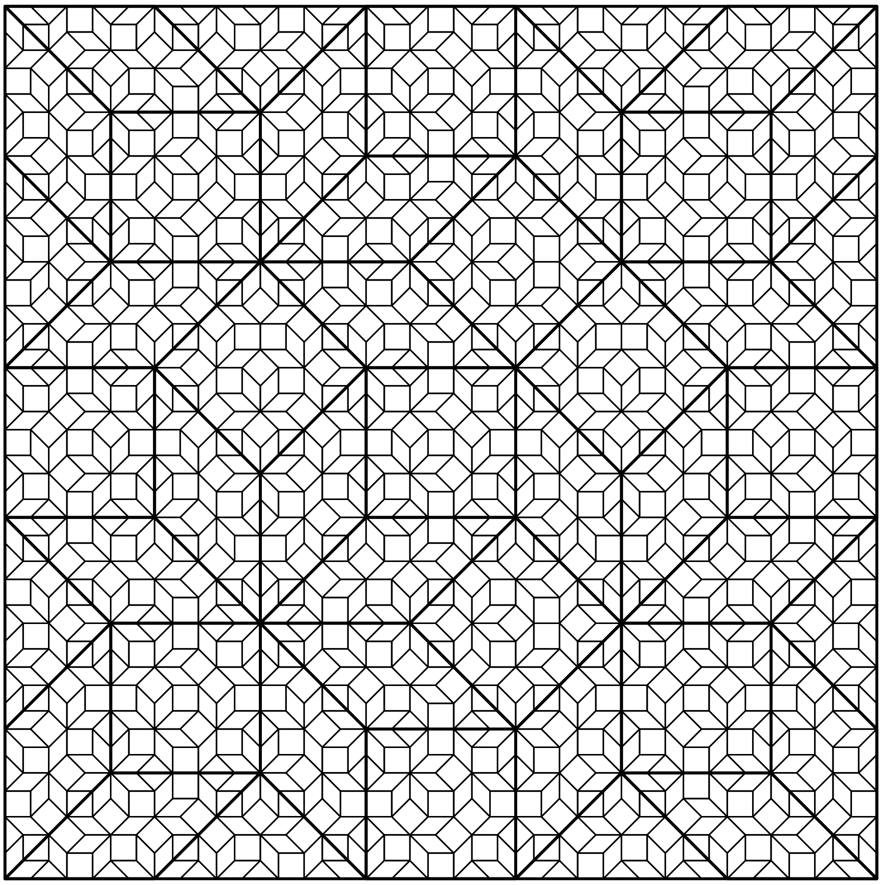

Fig. 12. Octagonal Ammann-Beenker tiling, subdivided into super-tiles

4 Octagonal Ammann-Beenker Tilings

4.1 The Alternation condition

In many respects, the octagonal Ammann-Beenker tiling [28,29], shown in Fig. 12, is among the simplest of all quasiperiodic tilings. To some extent, this is true also for its cluster descriptions. We shall therefore use it as our second example to illustrate the general principles of cluster models. Matching rules enforcing a perfect octagonal tiling are rather complicated [6,7,29]. They are expressed in terms of a complicated, non-local decoration of the tiling. However, there is a simple, local subset of the matching rules, which can easily be enforced with a cluster density maximization principle, or with a cluster covering principle. This subset of the matching rules is the alternation condition [20]. It requires that along any lane of tiles, the two types

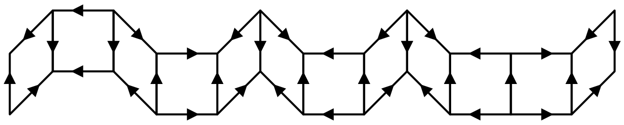

Fig. 13. The alternation condition requires that along a lane of tiles the two kinds of rhombi alternate. It can be enforced by an arrowing of the tiles

of rhombi must alternate, as illustrated in Fig. 13. The alternation condition can be enforced by a suitable arrowing of the tile edges. Opposite edges of squares have the same arrow direction, whereas opposite edges of rhombi have opposite arrow directions. The alternation condition cannot enforce octagonal tilings, but it does enforce *perfectly ordered*, quasiperiodic tilings, which are at least four-fold symmetric [21]. In fact, tilings satisfying the alternation condition are all members of a one-parameter family of four-fold symmetric, quasiperiodic tilings. The unique member of this family with even eight-fold symmetry is the Ammann-Beenker tiling. The square-rhombus tilings satisfying the alternation condition can be constructed by dualisation [28,43,44] of two superimposed square grids, which are rotated by 45° with respect to each other. These two square grids may have different scales, so that the resulting tiling is only four-fold symmetric in the general case. If the two grids have the same scale, the octagonal Ammann-Beenker tiling is obtained.

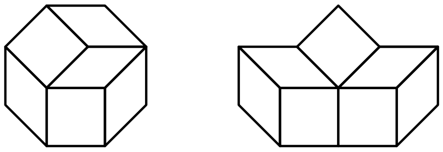

Fig. 14. Octagon and ship clusters favouring the alternation condition

A cluster density maximization principle can now be implemented in the following way. In a first step, one selects suitable clusters whose presence favours the alternation condition. Maximizing the density of these clusters with suitable weights will produce a tiling satisfying the alternation condition. In a second step, the weights of these favoured clusters are further tuned in such a way that the octagonal tiling has the highest weighted cluster density among all tilings satisfying the alternation condition. This program has been carried out with the clusters shown in Fig. 14 [22], which clearly favour the alternation condition. They have been selected with the goal that two rhombi which are neighbors along a lane of tiles are always covered by such a cluster (note that two such rhombi are never separated by more than two squares). For the second step, we need to compute the densities of these clusters for an arbitrary square-rhombus tiling satisfying the alternation condition. We note that the clusters can all be assigned to a unique super-tile (Fig. 12), and that super-tiles of the same type always carry the same number of clusters. In particular, for each super-tile square we have 14 octagon clusters and 3 ship clusters, and for each super-tile rhombus we have 10 octagon clusters and 2 ship clusters. The cluster densities are therefore a simple function of the super-tile densities. The latter, on the other hand, are easily obtained from the construction as the dual of two superimposed square grids. We simply have to compute the densities of gridline intersections of each type, suitably normalized by the total area of the corresponding tiles. If we denote by $1+x$ the ratio of the grid line spacings of the two square grids, we obtain in suitable units:

$$\rho_{\text{oct}}(x) = \frac{1+(1+x)^2}{(2+x)^2} \tag{4}$$

$$\rho_{\text{ship}}(x) = \frac{2\sqrt{2}(1+x)}{(2+x)^2} \tag{5}$$

For the octagonal tiling at $x = 0$, $\rho_{\text{oct}}(x)$ has a maximum, but $\rho_{\text{ship}}(x)$ has a minimum there. However, the weighted cluster density

$$\rho(x) = w_{\text{oct}}\rho_{\text{oct}}(x) + w_{\text{ship}}\rho_{\text{ship}}(x) \tag{6}$$

has a maximum at the octagonal point $x = 0$, provided

$$\frac{2\,w_{\text{oct}}}{w_{\text{ship}}} > \sqrt{2}+1. \tag{7}$$

This latter condition on the cluster weights is sufficient for the octagonal tiling to have the highest weighted cluster density among all tilings satisfying the alternation condition. But how about other tilings? Indeed, there are tilings having a higher octagon density than the octagonal tiling, but which do not satisfy the alternation condition. In order that these do not have a higher weighted cluster density, the relative weight of the ship cluster must not be to small. Monte Carlo simulations have shown [22] that the most extreme case is the periodic tiling made of super-tile rhombi only. In order to exclude also unwanted tilings which do not satisfy the alternation condition, the cluster weights must satisfy the double inequality

$$\sqrt{2}+1 < \frac{2\,w_{\text{oct}}}{w_{\text{ship}}} < (\sqrt{2}+1)^5. \tag{8}$$

Extensive Monte Carlo simulation have shown that whenever the cluster weights satisfy these inequalities, the octagonal Ammann-Beenker tiling has the highest weighted cluster density among all tilings [22]. At the upper bound, the periodic tiling with only super-tile rhombi becomes competitive, whereas at the lower bound, the periodic tiling with only super-tile squares becomes competitive. We should emphasize that the interval of allowed cluster weight ratios is very large, which makes this model very robust.

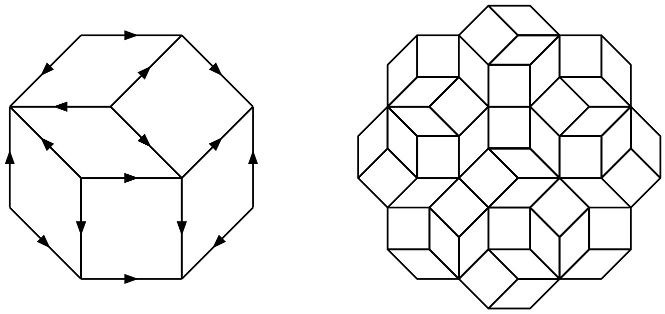

Fig. 15. Arrowed octagon cluster, and inflated unarrowed octagon cluster. Both impose the same overlapping constraints

If only the density of octagons is maximized, but the tile stoichiometry is fixed, then the set of tilings with maximal octagon density includes all super-tile random tilings with the given stoichiometry. In Fig. 12 one can see that super-tiles can be reshuffled without changing the number of octagons. We therefore obtain in this case a super-tile random tiling as ground state with maximal octagon density [22]. Tilings in such a super-tile random tiling ensemble look perfect at a local scale, but are disordered at larger scales. They can still be the basis of reasonable models for realistic quasicrystals.

The cluster density maximization model discussed above has the disadvantage that it needs two clusters, whose weights must satisfy certain constraints. This can be avoided [23] by arrowing the octagon cluster (Fig. 15). A tiling completely covered by the arrowed octagon must necessarily satisfy the alternation condition, and among these the Ammann-Beenker tiling has the highest octagon density. Under the assumption that tilings that are not completely covered by the arrowed octagon cannot have a higher arrowed octagon density than the maximal density for tilings that are covered, maximizing the density of the arrowed octagon can therefore enforce the octagonal Ammann-Beenker tiling. Although there is no proof for the above assumption, it appears highly plausible. In any case, the arrowed Ammann-Beenker tiling is ideally suited for the maximal cluster covering principle. It has the highest arrowed octagon density among all tilings that are covered by the arrowed octagon.

4.2 An Atomic Model for Octagonal Mn-Si-Al

In Sect. 4.1 we have seen that arrowed octagon clusters can be used with a maximal cluster covering principle to obtain the Ammann-Beenker tiling. If undecorated clusters are preferred for some reason, one could inflate the octagon once to arrive at a larger cluster, which has exactly the same asymmetries as the arrowed octagon (Fig. 15). This larger, undecorated cluster therefore imposes the same overlapping constraints, and can be used in place of the arrowed octagon. However, real quasicrystals are not tilings, but are at best decorations of a tiling. The tiling therefore has to be decorated with atoms, and it could also be this atomic decoration which introduces the necessary asymmetry, and thus imposes the necessary overlapping constraints.

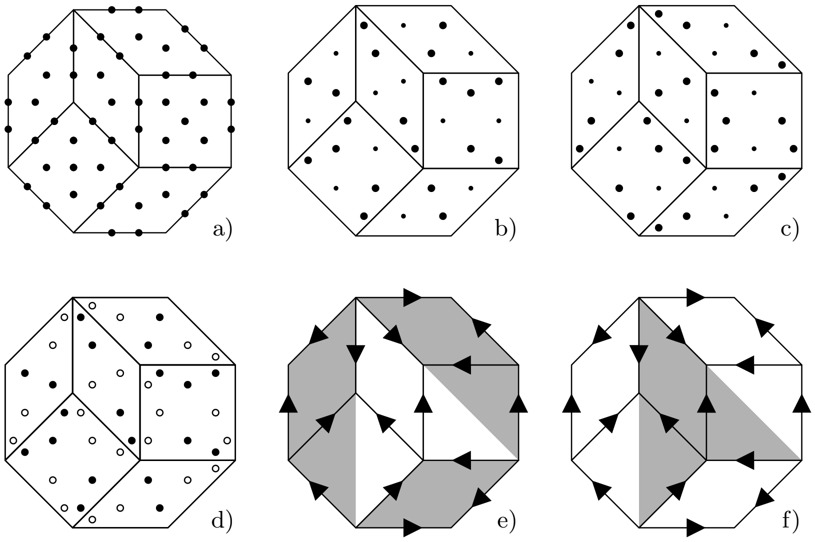

Fig. 16. Decoration of a small octagon patch. **a)** layer A, **b)** layer B, **c)** layer B', and **d)** layers B and B' together. Large dots denote Mn atoms, small dots Si or Al atoms. In d), only Mn atoms are shown; atoms from the B layer are shown as full dots, and atoms from the B' layer as open dots. In **e)** and **f)**, abstract representations of the layer stackings $ABAB'$ and $AB'AB$ are given, respectively

This is indeed the case for the quasicrystal structure of octagonal Mn-Si-Al described by Jiang, Hovmöller and Zhou [45], as has been discussed in detail in [46]. This quasicrystal is a layered structure $\ldots ABAB' \ldots$, and can be regarded as a decoration of the Ammann-Beenker tiling. The decoration of the octagon motifs (which cover the whole structure) is shown in Fig. 16. Both the decoration of the edges in layer A and the decoration of the interiors of the squares in layers B and B' show the same asymmetry as the arrowing. There are actually two possible decorations of an octagon, whose only difference is that the decorations of the layers B and B' are exchanged. One kind of octagon is decorated with a stacking $\ldots ABAB' \ldots$, the other with a stacking $\ldots AB'AB \ldots$. Since each octagon actually represents an infinite prism with octagonal base, these two decorations correspond to prisms which are translated by half a lattice period in the z-direction with respect to one another, but are identical otherwise. We therefore have a covering by identical prisms, which, of course, can be chopped into identical, finite clusters.

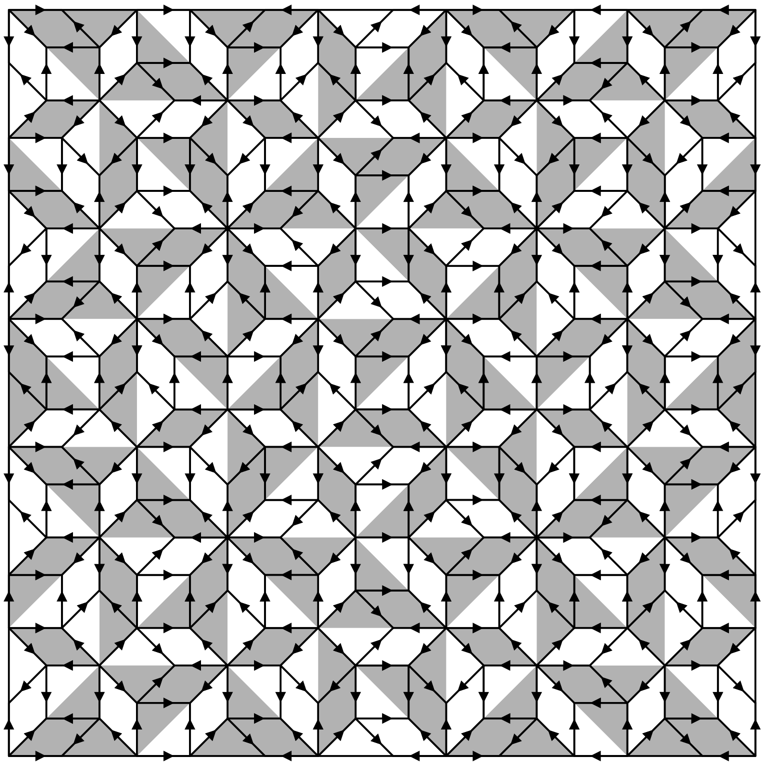

Fig. 17. Colored and arrowed Ammann-Beenker tiling

It is most convenient to represent these prisms again by an abstract decoration of the octagon. The different vertical positions of the prisms are encoded by a coloring, as shown in Figs. 16e,f. Tiles which differ in color, but have otherwise the same decoration, correspond to prisms shifted by half a lattice period in the z-direction. It is interesting to note that since the octagonal prisms occur at two different positions in the z-direction, the Bravais lattice of this octagonal quasicrystal must be an octagonal centered one [46]. This can also be seen in the colored and arrowed tiling of Fig. 17: if a tile is a translate of another tile by an odd number of tile edges, it has the opposite color. If an even number of tile edges separates the two tiles, they have like colors. In order to obtain a lattice translation, a (horizontal) translation by an odd number of tile edges must be combined with a translation in the z-direction by half a lattice period, in order to make up for the color change. This results in the octagonal centered lattice.

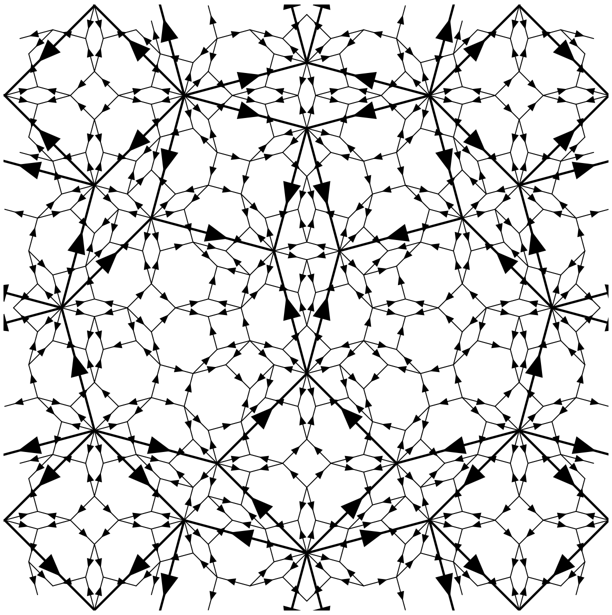

Fig. 18. The Socolar tiling, with superimposed super-tile tiling

5 Dodecagonal Socolar and Shield Tilings

5.1 The Socolar Tiling

The case of the dodecagonal Socolar tiling [6] (Fig. 18) is very analogous to that of the octagonal Ammann-Beenker tiling. This tiling can be obtained by the projection method, or as the dual of two superimposed triangular grids [44]. Like the Ammann-Beenker tiling, it satisfies an alternation condition [20]: along any lane of tiles, the two kinds of rhombi have to alternate (Fig. 19). This alternation is enforced by the arrowing of the tile edges. Besides the alternation condition, there is a further local constraint satisfied by the Socolar tiling. This becomes apparent if an inflated tiling is superimposed (Fig. 18). The edges of the inflated tiles have an asymmetric environment. There is a dodecagon cluster which is either on the right or on the left of the edge. We may say that square edges buckle inwards, rhombus edges buckle outwards, and the hexagon has opposite edges of different type. In order that an arrowed tiling by hexagons, squares and rhombi can be inflated, it must satisfy the local constraint that outward-buckling edges match only inward-buckling edges, and vice versa. This local constraint will henceforth be called the buckling constraint. Note that the edge types break the single mirror line of the arrowed hexagon, so that there are now left hexagons and right hexagons. Taking the buckling into account, arrowed hexagons are thus completely asymmetric. They then have exactly the same asymmetry as inflated

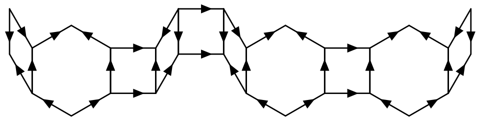

Fig. 19. The alternation condition for the Socolar tiling

hexagons. A tiling satisfying both the alternation condition and the buckling constraint can be inflated infinitely often.

Recall that in the case of the Ammann-Beenker tiling, the alternation condition enforces ordered tilings of at least four-fold symmetry. A closer analysis of the proof of Katz [21] shows that an analogous statement holds for the Socolar tiling [47]. One can show that every hexagon-square-rhombus tiling satisfying the alternation condition and the buckling constraint is quasiperiodically ordered and at least six-fold symmetric. More precisely, such a tiling is the dual of two superimposed triangular grids, which are rotated by 90° with respect to each other. These triangular grids may have different scales, so that the symmetry of the tiling is only hexagonal in general. If the scale of the two grids is the same, the dodecagonal Socolar tiling is obtained. This implies that all tilings admitted by the alternation condition and the buckling constraint are quasiperiodic (or periodic) and at least hexagonally symmetric. The simplest such tiling is the one with only hexagons.

5.2 Cluster Covering and Cluster Densities

The two tile clusters shown in Fig. 20 cover the entire Socolar tiling. This is best seen at the level of the superimposed super-tile tiling. Since super-tiles of a given shape all have the same decoration with small tiles, one just has to show that all super-tiles are covered. The dodecagon cluster alone covers already most of the tiling. The only bits that remain uncovered are a little square inside each big square, and a little hexagon and three little squares inside each big hexagon. There is one dodecagon cluster center near the middle of each super-tile edge (but not directly on the edge). Every dodecagon cluster can be assigned to a unique super-tile. There are two dodecagon clusters per super-tile rhombus, and three per super-tile hexagon. Super-tile squares are not assigned any dodecagon clusters. The remaining uncovered bits of the tiling are then covered by the butterfly cluster (Fig. 20). There is one butterfly cluster per super-tile square, and one per super-tile hexagon. Each of the two clusters occurs always with exactly the same decoration in the tiling. Since they are arrowed, every tiling that is covered by the clusters must necessarily satisfy the alternation condition, and due to the structure of the clusters the same must be the case also for the buckling constraint. Using the results of Sect. 5.1, we now know that every tiling that is covered by the two clusters is a quasiperiodic super-tile tiling of at least hexagonal symmetry.

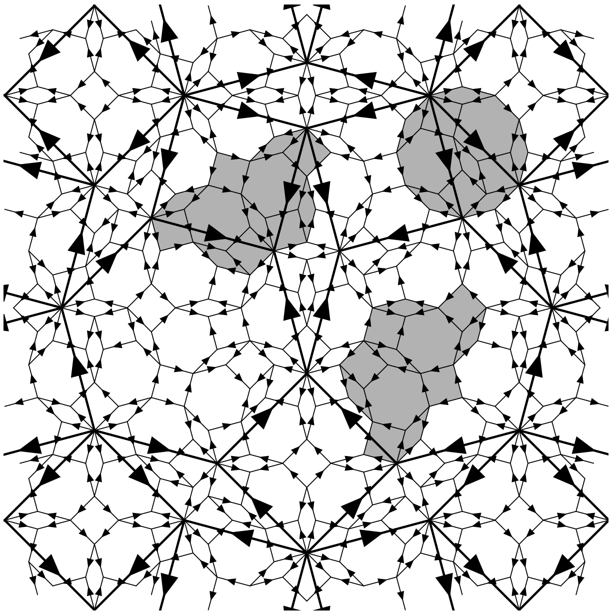

Fig. 20. The Socolar tiling, with superimposed super-tile tiling, and clusters indicated in gray

It remains to prove that among these tilings, the dodecagonal one has the highest cluster density. Recall that each cluster is assigned to a unique super-tile, and each such super-tile of a given kind carries the same number of clusters. Moreover, the super-tile tiling is the dual of two superimposed triangular grids, so that we can compute the densities of the super-tiles, which are parametrized by the ratio $1+x$ of the gridline spacings of the two grids. This parametrization is chosen such that the dodecagonal tiling corresponds to $x = 0$. From these super-tile densities, it is then easy to compute the cluster densities. In suitable units, we obtain:

$$\rho_{\mathrm{dod}}(x) = \frac{(6\sqrt{3}+48)(1+x)+3\sqrt{3}x^2}{1+x+x^2/6} \tag{9}$$

$$\rho_{\mathrm{bfl}}(x) = \frac{(2\sqrt{3}+6)(1+x)+\sqrt{3}x^2}{1+x+x^2/6} \tag{10}$$

$\rho_{\mathrm{dod}}(x)$ has a maximum for $x = 0$, but $\rho_{\mathrm{bfl}}(x)$ has a minimum there. However, the weighted cluster density

$$\rho(x) = w_{\mathrm{dod}}\rho_{\mathrm{dod}}(x) + w_{\mathrm{bfl}}\rho_{\mathrm{bfl}}(x) \tag{11}$$

has a maximum at the dodecagonal point $x = 0$, provided the weights satisfy the mild condition $w_{\mathrm{bfl}}/w_{\mathrm{dod}} < 12 + 10\sqrt{3}$.

We have therefore shown that square-hexagon-rhombus tilings that are completely covered by the dodecagon and the butterfly cluster satisfy the alternation condition and the buckling constraint. They are thus quasiperiodic and hexagonally symmetric. Among these tilings, the dodecagonal Socolar tiling has the highest weighted cluster density, provided a mild constraint on the cluster weights is satisfied. The dodecagonal Socolar tiling can therefore be obtained with a simple maximal cluster covering principle. This does not rigorously rule out the possibility that there are tilings which are not completely covered, but have an even higher weighted cluster density. Such a scenario seems rather unlikely, however.

These results are very similar to those for the Ammann-Beenker tiling. There is one key difference, however. For the dodecagonal Socolar tiling we need two covering clusters, whereas for the octagonal tiling (as well as for the Penrose tiling) one cluster was sufficient. By taking one larger cluster, it is possible to reduce the fraction of the uncovered area, even as far as one wants [48], but it does not seem possible to cover the whole tiling with one cluster of finite size. Whether such an almost covering can enforce an ordered tiling is unkown, however.

5.3 The Shield Tiling

Like there are several kinds of Penrose tilings which are all MLD with each other, there exists also for the Socolar tiling a whole family of other tilings which are MLD with it [49]. Since matching rules can be transferred between different tilings which are MLD [35], the same should also be possible with cluster coverings.

An interesting tiling which is MLD with the Socolar tiling is the shield tiling [30,31], which is shown in Fig. 21, together with the Socolar tiling. A closer inspection of Fig. 21 makes it evident how these two tilings are related to each other, and that this relation is a local equivalence relation. The Socolar tiling has as vertices the triangle centers of the shield tiling, and also the shield tiling is easily constructed from the Socolar tiling.

This local equivalence relation can even be extended to a larger class of tilings. On the one side, we have generalized Socolar tilings, and on the other side, we have generalized shield tilings. For simplicity, we shall call these also just Socolar tilings and shield tilings, respectively. On the Socolar tiling side, this larger class consists of all those tilings which satisfy the local constraint on the buckling of edges (Sect. 5.1). This constraint is essential in order that an equivalent shield tiling can be derived. To each edge of the Socolar tiling corresponds a vertex of the shield tiling, which is located on that side of the edge which is opposite to the buckling. Conversely, a shield tiling must satisfy the local condition that all squares and shields must be completely surrounded by triangles and double-triangles, and all triangles and double-triangles must be completely surrounded by squares and shields. Since the corresponding Socolar tiling has its vertices in the triangle centers of the

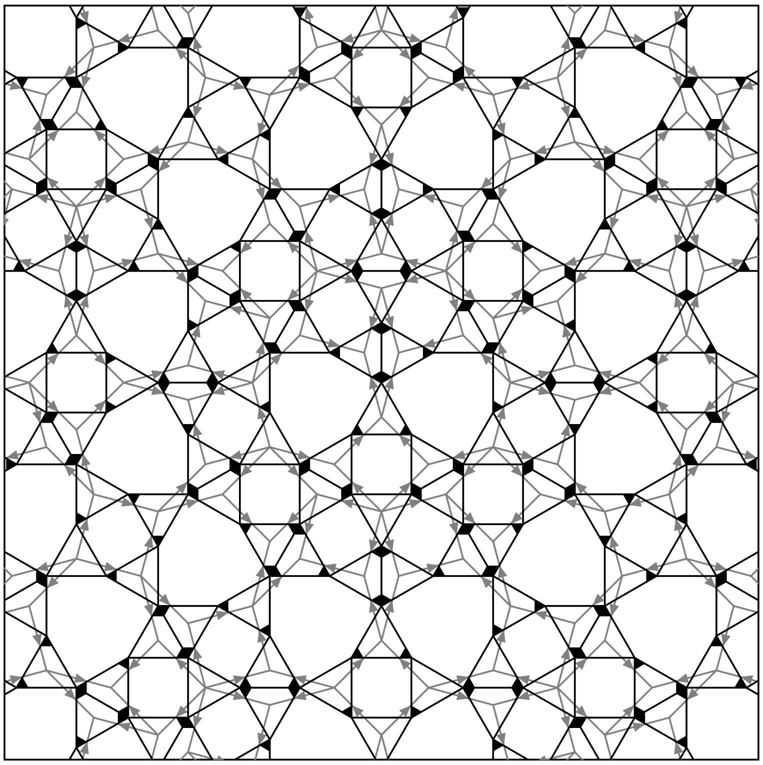

Fig. 21. The shield tiling, with associated Socolar tiling in gray

shield tiling, one would otherwise obtain new tile types in the corresponding Socolar tiling. When deriving the Socolar tiling from such a shield tiling, the Socolar tiling then automatically satisfies the edge buckling constraint. The generalized Socolar and shield tilings are therefore MLD, with the same derivation rules as the perfect tilings.

An interesting subset of the generalized Socolar tilings are those which satisfy the alternation condition. To this subset there exists also a corresponding subset of generalized shield tilings, so that by local derivation we can define the alternation condition also for the generalized shield tilings. Unfortunately, for the shield tilings it is not so easy to recognize directly whether the alternation condition is satisfied. We therefore have added in Fig. 21 marks to the vertices of the shield tiling, whose purpose is to encode the arrow direction of the nearby bond of the corresponding Socolar tiling.

We are now ready to define the covering clusters also for the shield tiling. These clusters, shown in Fig. 22, are directly derived from the corresponding clusters of the Socolar tiling. Their decoration with marks at the vertices has the purpose to ensure that any tiling covered by them satisfies the alternation condition. In order that this works, the following overlap rules have to be

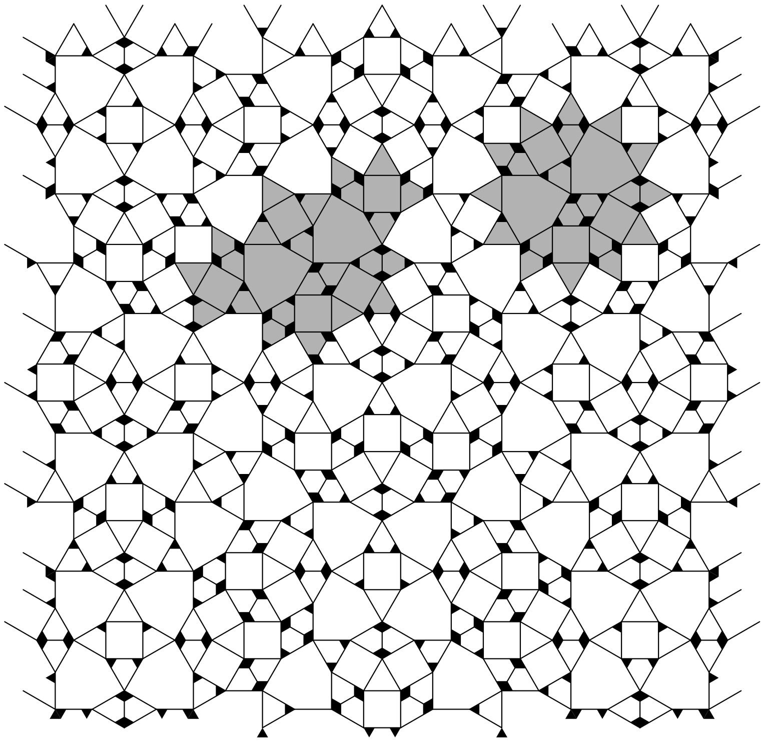

Fig. 22. The shield tiling, with clusters indicated in gray

applied. Two overlapping clusters are compatible with each other if all tiles in the overlap agree, and if all marks in the overlap agree, except perhaps those at the outermost triangle vertices of the clusters. Without this latter exception one would have to introduce further types of clusters. These overlap rules then ensure that any tiling completely covered by the clusters is a generalized shield tiling satisfying the alternation condition, and therefore is locally equivalent to a generalized Socolar tiling satisfying the alternation condition. Since the two are locally equivalent, also the cluster densities are the same, and so we can easily transfer all results we have obtained for the Socolar tiling also to the shield tiling. In other words, also the dodecagonal shield tiling can be obtained with a maximal cluster covering principle, where the same weighted cluster density has to be used as for the Socolar tiling.

6 Voronoi and Delone Clusters

In recent papers [50–53], Kramer has argued that the existence of covering clusters should be expected for theoretical reasons, at least for the canonical projection tilings. There are two kinds of such projection tilings [54]. The first kind has vertices at projected lattice positions, with an acceptance domain which is the projected Voronoi cell of the higher-dimensional lattice. The second kind has vertices at projected corners of the Voronoi cells, with acceptance domains which are the projected, dual Delone cells. According to this theory, for the first kind of canonical projection tilings we should expect covering clusters at projected corners of Voronoi cells, whose size is given by the corresponding projected Delone cell. Conversely, for the second kind of canonical projection tilings, covering clusters are expected at projected lattice points, with a size given by the projected Voronoi cell. In other words, covering clusters and vertices are, in a sense, dual to each other. There does not seem to be a proof that Voronoi or Delone clusters indeed cover the whole tiling without gaps in the general case, but for many particular examples this has been verified.

Indeed, the examples discussed in the previous sections are exactly of this kind. The aperiodic decagon covering the Penrose (rhombus) tilings is centered at projected lattice points, whereas the vertices of the Penrose tiling are at projected corners of the Voronoi cells. In the case of the octagonal Ammann-Beenker tiling, the vertices are at projected lattice points, whereas the octagon cluster is centered at projected corners of the Voronoi cells. In the case of the dodecagonal Socolar tiling, the dodecagon cluster is again of this kind. It is centered at projected lattice points, whereas the vertices of the Socolar tiling are projected corners of Voronoi cells. Only the butterfly cluster does not really fit into this picture. In all these cases, the cluster size coincides with the size predicted by theory.

Kramer has discussed in detail a further example, the Tübingen-Triangle-Tiling (TTT) [50,52]. Here, the clusters are located at projected corners of the Voronoi cells, whose sizes correpond to projected Delone cells. There are four translation classes of cluster centers, and thus also four different clusters, two small and two big pentagons. Disregarding orientation, there are just two clusters, big and small pentagons (Fig. 23), which indeed cover the TTT [52].

Unfortunately, obtaining the TTT by means of a cluster covering principle, or a maximal cluster covering principle, seems much more difficult. Like the Ammann-Beenker and Socolar tilings, the TTT has rather complicated

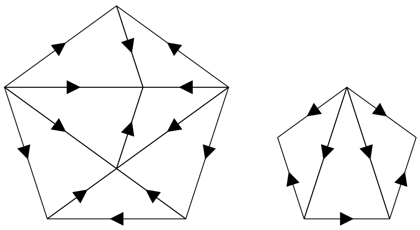

Fig. 23. Pentagon clusters covering the arrowed Tübingen Triangle Tiling. Both clusters, as well as their mirror images, occur in 10 orientations

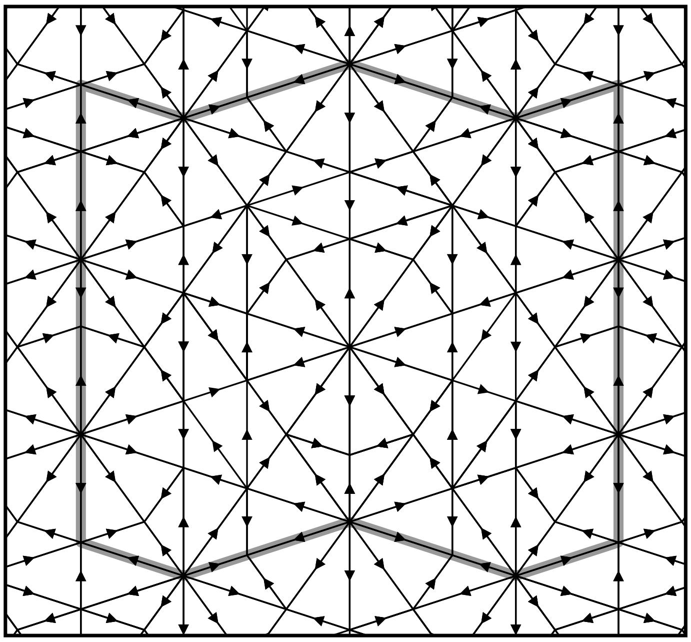

Fig. 24. Cluster covering of a periodic variant of the Tübingen-Triangle-Tiling. A unit cell is outlined in gray

matching rules, at least if one insists on short-range matching rules [8]. It is therefore rather difficult to encode these matching rules in terms of overlap rules for a small number of simple clusters. The matching rules can be formulated in terms of two kinds of decorations of the tiling, edge decorations and vertex decorations [8]. The edge decorations can easily be incorporated into the pentagon clusters (Fig. 23). The edge decoration alone is not enough, however, to enforce a quasiperiodic tilings. It helps to avoid that even the simplest periodic tilings can be covered by the clusters as well, but there are still more complicated periodic approximants that are also covered by the clusters. One such approximant is shown in Fig. 24. There are wrong cluster arrangements around the center of the decagons formed by ten big triangles. The vertex decoration of the matching rules would not allow these, but if such vertex decorations are introduced, each cluster splits into several subvariants, which differ in their decoration. All this suggests that there is no *simple* cluster model that could enforce a perfectly ordered TTT. This shows that the mere existence of simple covering clusters is not enough to enforce an ordered structure. There still is the possibility that applying a covering principle at *fixed stoichiometry* may select an interesting class of super-tile random tilings, like for the relaxed decagon overlap rules in the Penrose case, but this has not been worked out so far.

References

1. S. Burkov: Phys. Rev. Lett. **67**, 614 (1991)
2. H.-C. Jeong, P.J. Steinhardt: Phys. Rev. Lett. **73**, 1943 (1994)
3. C.L. Henley, 'Matching Rules for Quasiperiodic Tilings'. In: *Quasicrystals: The state of the Art*, ed. by D.P. DiVincenzo, P.J. Steinhardt (World Scientific, Singapore 1991), pp. 185–212
4. L.S. Levitov: Commun. Math. Phys. **119**, 627 (1988)
5. N.G. de Bruijn: Ned. Akad. Wetensch. Proc. Ser. A **43**, 39, 53 (1981)
6. J.E.S. Socolar: Phys. Rev. B**39**, 10519 (1989)
7. F. Gähler: J. Non-Cryst. Solids **153&154**, 160 (1993)
8. R. Klitzing, M. Baake, M. Schlottmann: Int. J. Mod. Phys. B **7**, 1455 (1993)
9. Y. Yan, S.J. Pennycook: Phys. Rev. Lett. **86**, 1542 (2001)
10. F. Gähler: Phys. Rev. Lett. **74**, 334 (1995)
11. P. Gummelt: 'Construction of Penrose Tilings by a Single Aperiodic Protoset'. In: *Quasicrystals, 5th International Conference at Avignon, France, May 22–26, 1995*, ed. by C. Janot, R. Mosseri (World Scientific, Singapore 1995) pp. 84–87
12. P. Gummelt: Geometriae Dedicata **62**, 1 (1996)
13. P.J. Steinhardt, H.-C. Jeong, K. Saitoh, M. Tanaka, E. Abe, A.P. Tsai: Nature **396**, 55 (1998)
14. R. Wittmann: Z. Kristallogr. **214** (1999) 501
15. E. Abe, T.J. Sato, A.P. Tsai: Phys. Rev. Lett. **82**, 5269 (1999)
16. E. Cockayne, Mat. Sci. Eng. A **294–296**, 224 (2000)
17. E. Abe, K. Saitoh, H. Takakura, A.P. Tsai, P.J. Steinhardt, H.-C. Jeong: Phys. Rev. Lett. **84**, 4609 (2000)
18. H.-C. Jeong, P.J. Steinhardt: Phys. Rev. B **55**, 3520 (1997)
19. M. Baake, M. Schlottmann, P.D. Jarvis: J. Phys. A: Math. Gen. **24**, 4637 (1991)
20. J.E.S. Socolar: Commun. Math. Phys. **129**, 599 (1990)
21. A. Katz: 'Matching Rules and Quasiperiodicity: The Octagonal Tilings'. In: *Beyond Quasicrystals*, ed. by F. Axel, D. Gratias (Les Editions de Physique and Springer, Les Ulis/Heidelberg 1995) pp. 141–189
22. F. Gähler, H.-C. Jeong: J. Phys. A: Math. Gen. **28**, 1807 (1995)
23. F. Gähler: 'Cluster Interactions for Quasiperiodic Tilings'. In: *Quasicrystals, 5th International Conference at Tokyo, Japan, May 26–30, 1997*, ed. by S. Takeuchi, T. Fujiwara (World Scientific, Singapore 1998) pp. 95–98
24. F. Gähler, R. Lück, S.I. Ben-Abraham, P. Gummelt: Ferroelectrics **250**, 335 (2001)
25. C.L. Henley, 'Random Tiling Models'. In: *Quasicrystals: The state of the Art*, ed. by D.P. DiVincenzo, P.J. Steinhardt (World Scientific, Singapore 1991), pp. 429–524
26. P. Gummelt, C. Bandt: Mat. Sci. Eng. A **294–296**, 250 (2000)
27. F. Gähler, M. Reichert: to appear in J. Alloys Comp. (2002)
28. F.P.M. Beenker, TH Report 82-WSK-04 (Technische Hogeschool, Eindhoven, 1982)
29. R. Ammann, B. Grünbaum, G.C. Shephard: Discrete Comput. Geom. **8**, 1 (1992)
30. F. Gähler: 'Crystallography of Dodecagonal Quasicrystals'. In: *Quasicrystalline Materials*, ed. by Ch. Janot, J.M. Dubois (World Scientific, Singapore 1988) pp. 272–284

31. K. Niizeki, H. Mitani: J. Phys. A: Math. Gen. A **20**, L405 (1987)
32. M. Baake, P. Kramer, M. Schlottmann, D. Zeidler: Int. J. Mod. Phys. B **4**, 2217 (1990)
33. F. Gähler: 'Cluster Coverings: A Powerful Ordering Principle for Quasicrystals'. In: *Quasicrystals: Current Topics*, ed. by E. Belin-Ferré, C. Berger, M. Quiquandon, A. Sadoc (World Scientific, Singapore 2000), pp. 118–127
34. F. Gähler: Mat. Sci. Eng. A **294–296**, 199 (2000)
35. F. Gähler, M. Baake, M. Schlottmann: Phys. Rev. B **50**, 12458 (1994)
36. M.E.J. Newman, G.T. Barkema: *Monte Carlo Methods in Statistical Physics*, Oxford University Press, New York 1999
37. B. Grünbaum, G.C Shephard: *Tilings and Patterns*, Freeman, New York, 1987
38. P. Gummelt: *Aperiodische Überdeckungen mit einem Clustertyp*, Shaker Verlag, Aachen 1999
39. L.-H. Tang, M.V. Jarić: Phys. Rev. **B 41**, 4524 (1990)
40. J. Lee: Phys. Rev. Lett. **71**, 211 (1993)
41. F. Gähler: 'Thermodynamics of Random Tiling Quasicrystals'. In: *Quasicrystals, 5th International Conference at Avignon, France, May 22–26, 1995*, ed. by C. Janot, R. Mosseri (World Scientific, Singapore 1995) pp. 236–239
42. J. Roth, C. L. Henley: Phil. Mag. A **75**, 861 (1997)
43. F. Gähler, J. Rhyner: J. Phys. A: Math. Gen. **19**, 267 (1986)
44. F. Gähler, P. Stampfli: Int. J. Mod. Phys. B **7**, 1333 (1993)
45. J.C. Jiang, S. Hovmöller, X.D. Zou: Phil. Mag. Lett. **71**, 123 (1995)
46. S.I. Ben-Abraham, F. Gähler: Phys. Rev. B **60**, 860 (1999)
47. F. Gähler, unpublished.
48. S.I. Ben-Abraham, P. Gummelt, R. Lück, F. Gähler: Ferroelectrics **250**, 313 (2001)
49. H.-U. Nissen: 'A Two-Dimensional Quasiperiodic Tiling by Two Pentagons'. In: *Quasicrystals, Networks, and Molecules of Fivefold Symmetry*, ed. by I. Hargittai (VCH Publishers, New York, 1990), pp. 181–199
50. P. Kramer: J. Phys. A: Math. Gen. **32**, 5781 (1999)
51. P. Kramer, Mat. Sci. Eng. A **294–296**, 401 (2000)
52. P. Kramer: J. Phys. A: Math. Gen. **33**, 7885 (2000)
53. P. Kramer: J. Phys. A: Math. Gen. **34**, 1885 (2001)
54. P. Kramer, M. Schlottmann: J. Phys. A: Math. Gen. **22**, L1097 (1989)